

# Interactions, star formation and AGN activity

Cheng Li<sup>1,2\*</sup>, Guinevere Kauffmann<sup>2</sup>, Timothy M. Heckman<sup>3</sup>, Simon D.M. White<sup>2</sup>,  
Y. P. Jing<sup>1</sup>

<sup>1</sup>MPA/SHAO Joint Center for Astrophysical Cosmology at Shanghai Astronomical Observatory, Nandan Road 80, Shanghai 200030, China

<sup>2</sup>Max Planck Institut für Astrophysik, Karl-Schwarzschild-Strasse 1, 85748 Garching, Germany

<sup>3</sup>Department of Physics and Astronomy, Johns Hopkins University, Baltimore, MD 21218

Accepted ..... Received .....; in original form .....

## ABSTRACT

It has long been known that galaxy interactions are associated with enhanced star formation. In a companion paper, we explored this connection by applying a variety of statistics to SDSS data. In particular, we showed that specific star formation rates of galaxies are higher if they have close neighbours. Here we apply exactly the same techniques to AGN in the survey, showing that close neighbours are not associated with any similar enhancement of nuclear activity. Star formation is enhanced in AGN with close neighbours in exactly the same way as in inactive galaxies, but the accretion rate onto the black hole, as estimated from the extinction-corrected [O III] luminosity, is not influenced by the presence or absence of companions. Previous work has shown that galaxies with more strongly accreting black holes contain more young stars in their inner regions. This leads us to conclude that star formation induced by a close companion and star formation associated with black hole accretion are distinct events. These events may be part of the same physical process, for example a merger, provided they are separated in time. In this case, accretion onto the black hole and its associated star formation would occur only after the two interacting galaxies have merged. The major caveat in this work is our assumption that the extinction-corrected [O III] luminosity is a robust indicator of the bolometric luminosity of the central black hole. It is thus important to check our results using indicators of AGN activity at other wavelengths.

**Key words:** galaxies: clustering - galaxies: distances and redshifts - large-scale structure of Universe - cosmology: theory - dark matter

## 1 INTRODUCTION

In Li et al. (2007, hereafter Paper I) we used a variety of statistics to study the small-scale clustering properties of a sample of  $10^5$  star-forming galaxies selected from the data release 4 of the Sloan Digital Sky Survey (SDSS; York et al. 2000). We cross-correlated star-forming galaxies with reference samples drawn from the main spectroscopic survey and from the photometric catalogue (which is complete down to significantly fainter limiting magnitudes). We also calculated the average enhancement in star formation rate as a function of the projected distance to companion galaxies. Our results supported a picture in which enhanced star formation activity and galaxy interactions are closely linked. At the highest specific star formation rates, almost all galaxies were found to have a close companion or be in the process of merging. Galaxies with the highest specific star formation rates were

also found to be more concentrated, suggesting that these merger-driven interactions were building up their bulge components. These results are in accord with gas-dynamical simulations of mergers of disk galaxies, which show that substantial fraction of the gas in the galaxy can be driven towards the center of the galaxy by gravitational torques, where it can fuel a central starburst (Negroponte & White 1983; Mihos & Hernquist 1996).

The discovery of a tight correlation between black hole mass and bulge mass or velocity dispersion in galaxies (Gebhardt et al. 2000; Ferrarese & Merritt 2000) has motivated many theoretical models in which accretion onto black holes and AGN activity are assumed to be closely linked to galaxy interactions and mergers (see for example Kauffmann & Haehnelt 2000; Cattaneo 2001; Granato et al. 2001; Wyithe & Loeb 2002; Di Matteo et al. 2003; Cattaneo et al. 2005; Hopkins et al. 2005; Kang et al. 2005; Bower et al. 2006; Croton et al. 2006). In many of these models, a few per cent of the gas in the merging galaxy-

\* E-mail: leech@mpa-garching.mpg.de

ies is accreted by the black hole and shines with a radiative efficiency of around 10% over a time scale of a few  $\times 10^7$  years. With these simple assumptions, many of the observed features of the cosmological evolution of quasars appear to be reasonably well reproduced. It is therefore interesting to explore whether we can find any empirical evidence for a connection between merging and AGN activity in the real Universe. Previous observational studies have yielded contradictory results (see for example Petrosian 1982; Dahari 1984, 1985; Keel et al. 1985; Fuentes-Williams & Stocke 1988; Virani, De Robertis, & VanDalsen 2000; Schmitt 2001; Miller et al. 2003; Grogin et al. 2005; Waskett et al. 2005; Koulouridis et al. 2006; Serber et al. 2006). It is thus useful to carry out a careful analysis of a large and homogeneous sample of AGN.

In Li et al. (2006), we presented results on the clustering of AGN selected from the SDSS. Our study did not yield any evidence that AGN activity is triggered by interactions with nearby companions. Instead we found that AGN are clustered *more weakly* than control samples of non-AGN on scales between 100 kpc and 1 Mpc. We interpreted this anti-bias as evidence that AGN activity is favoured in galaxies that are located at the centres of their own dark matter halos, and disfavoured in “satellite galaxies” that orbit together with many other galaxies within a common halo.

The purpose of this short paper is to bring our results on star-forming galaxies and AGN together. We analyze star-forming galaxies and AGN in exactly the same way, using the same set of statistics, and we compare and contrast the results that are obtained for the two kinds of galaxy. We then discuss the implications of our results for understanding the connection between star formation, AGN activity and galaxy interactions

## 2 INDICATORS OF STAR FORMATION AND AGN ACTIVITY

Our basic indicator of star formation activity in galaxies is the *specific star formation rate*, which is defined as the star formation rate of the galaxy measured within the 3 arcsecond SDSS fibre aperture divided by the stellar mass of the galaxy measured within this same aperture. Extinction-corrected star formation rates are estimated using a variety of emission lines as described in Brinchmann et al. (2004).

Our indicator of AGN activity is the quantity  $L[\text{O III}]/M_{\text{BH}}$ , where  $L[\text{O III}]$  is the  $[\text{O III}]\lambda 5007$  emission line luminosity in solar units and  $M_{\text{BH}}$  is the black hole mass (in solar masses) estimated from the measured stellar velocity dispersion of the galaxy using the fitting formula provided by Tremaine et al. (2002). As discussed in Kauffmann et al. (2003, hereafter K03), the contribution to the  $[\text{O III}]$  luminosity from  $[\text{H II}]$  regions is small in nearby AGN. The  $[\text{O III}]$  line is expected to come almost exclusively from the narrow-line region, making it an excellent probe of accretion onto the central supermassive black hole. Additional support for the  $[\text{O III}]$  line luminosity as an accretion rate indicator is provided by the study of a hard X-ray selected sample of 47 AGN by Heckman et al. (2005), which showed that the 3–20 keV and  $[\text{O III}]$  luminosities were well-correlated over a range of about 4 orders of magnitude.

The main drawback of the  $[\text{O III}]$  emission line is that

it is affected by dust extinction. Hopkins et al. (2005) developed a model in which the lifetime and visibility of quasars is intimately connected with obscuration inside merging systems. In their model, mergers funnel gas to galaxy centres, fuelling starbursts and feeding black hole growth, but the quasars remain “buried” until accretion-related feedback disperses the obscuring material and they are revealed. Eventually, activity ceases as the remnants settle down and the accretion rate drops. In such a model obscuration effects vary dramatically as a system ages. Here, we attempt to correct the  $[\text{O III}]$  luminosity for dust obscuration using the value of the Balmer decrement measured from the galaxy spectrum (see K03). This is of course a crude correction, because the  $\text{H}\alpha$  and  $\text{H}\beta$  line fluxes are likely to be dominated by emission from  $\text{H II}$  regions that may be spread over a larger spatial scale than the gas clouds that contribute to high-ionization emission lines such as  $[\text{O III}]$ . Nevertheless, we believe that correcting for dust in this way will improve the correlation between our AGN activity indicator and the bolometric luminosity of the central black hole.

We note that the majority of AGN in our sample are relatively low-luminosity objects with  $[\text{O III}]$  line luminosities well below those of typical high-redshift quasars. Heckman et al. (2004) showed that high-mass black holes are accreting very little at the present day; only black holes of  $10^8 M_{\odot}$  or less continue to accrete and to grow at a significant rate. The SDSS optical AGN sample includes 4680 objects with  $\log L[\text{O III}]/M_{\text{BH}} > 1$ . This cut selects the  $\sim 5\%$  of our AGN sample with the most rapidly growing black holes. According to the calibration between  $[\text{O III}]$  line luminosity and accretion rate given in Heckman et al. (2004), and taking account the average extinction correction that we apply here to the  $[\text{O III}]$  line, the black holes in these galaxies are accreting at approximately a tenth of Eddington or more. Even though these AGN may have significantly lower  $[\text{O III}]$  luminosities than high-redshift quasars, they are as powerful as these quasars when their luminosities are expressed in Eddington units. We thus believe that they can provide valuable insight into the processes that are responsible for triggering strong AGN activity.

## 3 RESULTS

Our sample of star-forming galaxies is the same as described in Paper I. The sample of AGN used here is the same as in Li et al. (2006). In short, the parent sample is composed of 397,344 objects which have been spectroscopically confirmed as galaxies and have data publicly available in the SDSS Data Release 4 (Adelman-McCarthy et al. 2006). AGN and star-forming galaxies are selected from the subset of galaxies with  $S/N > 3$  in the four emission lines  $[\text{O III}]\lambda 5007$ ,  $\text{H}\beta$ ,  $[\text{N II}]\lambda 6583$  and  $\text{H}\alpha$ , following the criteria proposed by K03.

Our methodology for evaluating the clustering properties of these galaxies has already been described in Paper I, so we will turn directly to our results.

### 3.1 Cross-correlation functions

In Figure 1, we compare projected redshift-space 2-point cross-correlation functions (2PCF)  $w_p(r_p)$  for our sample

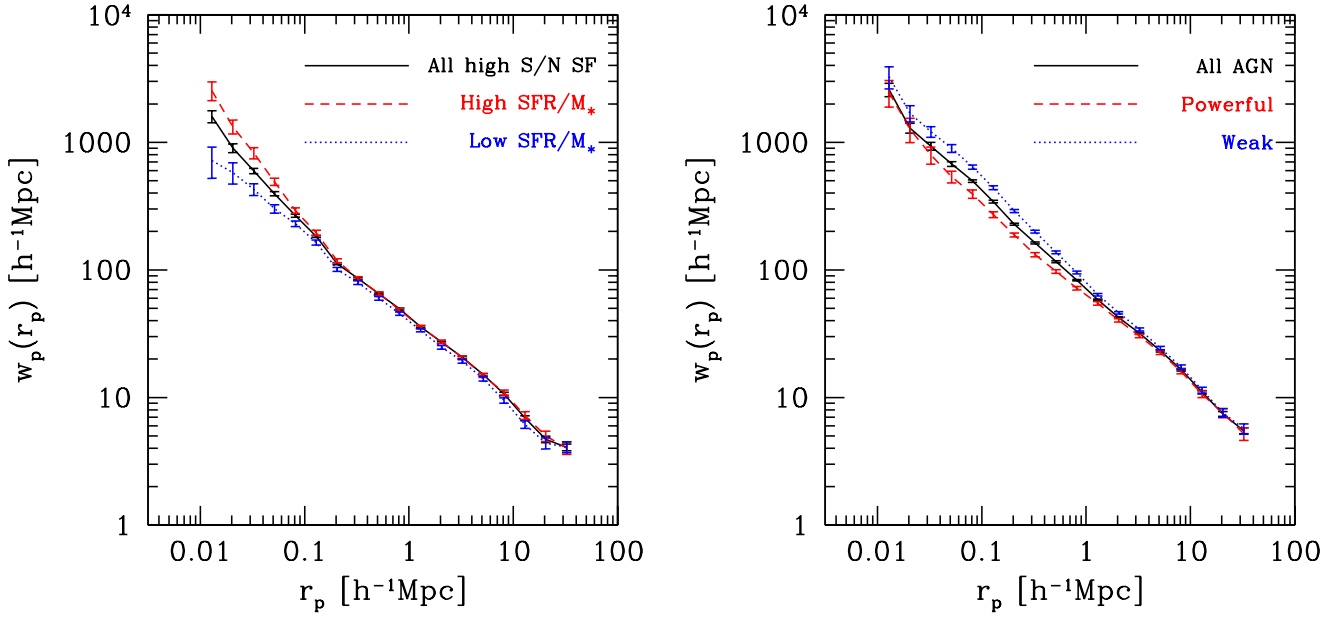


**Figure 1.** Projected redshift-space two-point cross-correlation functions  $w_p(r_p)$  between all high S/N star-forming galaxies and our reference sample (left) and between all AGN and our reference sample (right). Different lines correspond to star-forming galaxies with different specific star formation rates, or to AGN with different accretion rates, as indicated. See the text for a more detailed description.

of star-forming galaxies (left) and AGN (right). Results for the whole sample are plotted in black. Results for the 25% of galaxies with the smallest values of  $\text{SFR}/M_*$  and  $\text{L}[\text{O III}]/M_{\text{BH}}$  are plotted in blue. Results for the 25% of galaxies with the highest values of  $\text{SFR}/M_*$  and  $\text{L}[\text{O III}]/M_{\text{BH}}$  are plotted in red. The left panel shows that galaxies with high specific star formation rates are more strongly clustered than galaxies with low specific star formation rates on scales less than  $100 h^{-1}$  kpc and that the difference in clustering amplitude increases as one goes to smaller values of  $r_p$ . The right panel shows that AGN display quite different behaviour. AGN with the highest values of the Eddington parameter  $\text{L}[\text{O III}]/M_{\text{BH}}$  are *more weakly* clustered on scales between 30 kpc and 1 Mpc. At the smallest values of  $r_p$ , the clustering amplitude exhibits no dependence on AGN power.

These results are shown again in more detail in Figure 2, where we plot the amplitude of the 2PCF as a function of  $\text{SFR}/M_*$  and as a function of  $\text{L}[\text{O III}]/M_{\text{BH}}$  for three different values of the projected separation ( $r_p = 0.05, 0.5$  and  $5 h^{-1}$  Mpc). We extend the results to lower values of  $\text{SFR}/M_*$  using the sample of low S/N star-forming galaxies described in Paper I. It is interesting that the trends are qualitatively similar for the two kinds of object, except on the smallest scales where the clustering amplitude increases substantially for the large values of  $\text{SFR}/M_*$ , but exhibits no dependence on the Eddington parameter  $\text{L}[\text{O III}]/M_{\text{BH}}$ . We note that this lack of dependence extends up to the very highest values of  $\log \text{L}[\text{O III}]/M_{\text{BH}}$ , corresponding to black holes that are accreting at more than a tenth of the Eddington rate.

For both star-forming galaxies and AGN, the small-scale clustering amplitude increases strongly towards low values of  $\text{SFR}/M_*$  and  $\text{L}[\text{O III}]/M_{\text{BH}}$ . This is most likely

not a signature of mergers or interactions. In a recent paper, Barton et al. (2007) use cosmological N-body simulations to show that a substantial fraction of close galaxy pairs reside in cluster or group-size halos. It is well known that the star formation rates of galaxies are lower in these environments (e.g. Balogh et al. 1999), and the same is probably true of the average accretion rate onto the central black hole (K03). The upturn in clustering amplitude for galaxies with low values of  $\text{SFR}/M_*$  and for weak AGN is thus a signature of galaxies “shutting down” in the most massive halos.

### 3.2 Neighbour Counts

As in Paper I, we compute the number of galaxies in the photometric reference sample in the vicinity of star-forming galaxies and AGN and we make a statistical correction for the effect of chance projections. We have trimmed the AGN and star-forming samples so that they each have the same distribution in redshift and stellar mass. In Figure 3 we plot the average background-subtracted neighbour count within a given value of the projected radius  $r_p$ . Results are shown for star-forming galaxies in different intervals of  $\text{SFR}/M_*$  and AGN in different intervals of  $\log_{10}(\text{L}[\text{O III}]/M_{\text{BH}})$ . The photometric reference sample is always limited at  $r_{\text{pho}} = 20.0$ . We see a clear trend for an increase in the average number of close neighbours around the most strongly star-forming galaxies, but not around the most powerful AGN.

### 3.3 “Enhancement” functions

In Paper I, we computed the background-corrected, neighbour-count-weighted enhancement in specific star formation rate for galaxies as a function of projected neighbour

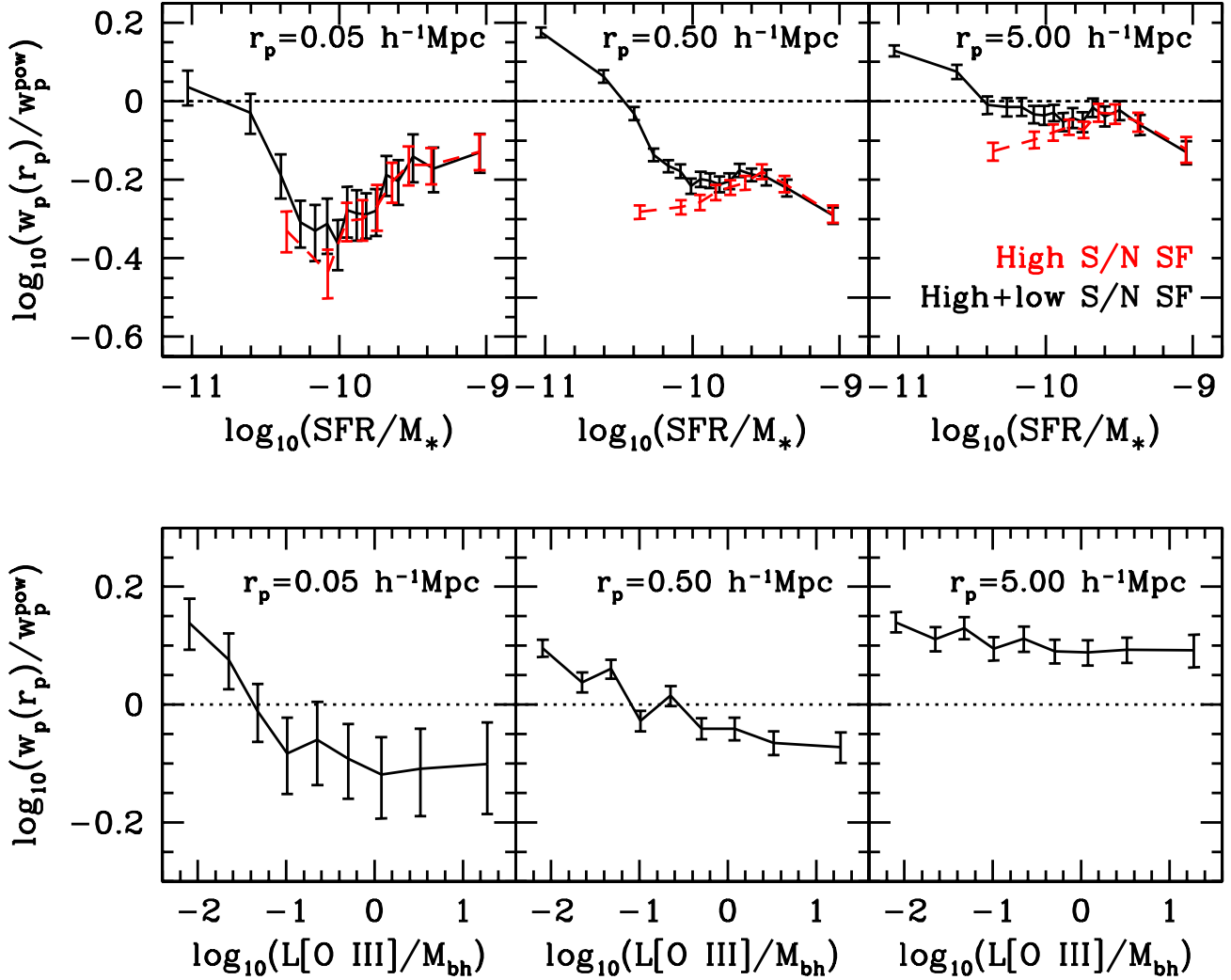


**Figure 2.** Projected two-point cross-correlations  $w_p(r_p)$ , normalized by the expectation for a power-law 3-D correlation function  $\xi(r) = (r/5h^{-1}\text{Mpc})^{-1.8}$  and measured at the  $r_p$  values indicated in each panel, are plotted as a function of  $\log_{10} \text{SFR}/M_*$  for star-forming galaxies (top panels) and as a function of  $\log_{10}(L[\text{O III}]/M_{\text{BH}})$  for AGN (bottom panels).

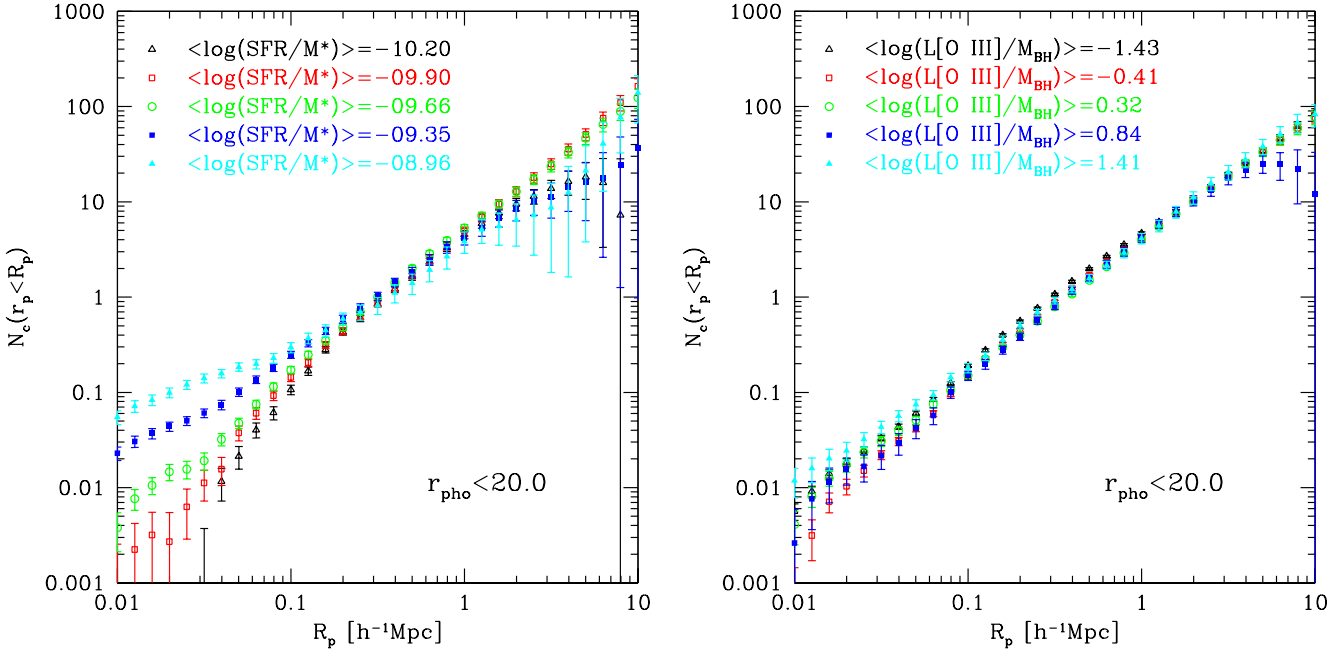
distance, The reader is referred to Paper I for definitions and for further details about the method.

Figure 4 compares the enhancement in specific star formation rate (left) with the enhancement in the level of nuclear activity, as measured by the quantity  $\log L[\text{O III}]/M_{\text{BH}}$  (right). The top panels show the enhancement functions as function of projected separation  $r_p$ , while in the bottom panel the separation is scaled by dividing by R90, the radius that encloses 90% of the  $r$ -band light of the galaxy.

As can be seen, AGN behave very differently to star forming galaxies. Accretion onto the black hole is *suppressed* for galaxies with companions with projected separations between  $\sim 100 \text{ kpc} - 1 \text{ Mpc}$ , and there is no evidence that the nuclear activity level is enhanced above the mean at small neighbour separations. The most plausible explanation for the suppression on intermediate scales is that the majority of AGN with close neighbours are located in groups and clusters and the suppression of nuclear activity is a larger-scale

environmental effect, similar to the morphology-density or SFR-density relations. This hypothesis is in accord with the AGN clustering model of Li et al. (2006), in which AGN activity is suppressed in satellite galaxies relative to central galaxies.

In Figure 5, we show how the enhancement functions depend on stellar mass for both the star-forming and the AGN samples. The suppression of AGN activity in galaxies with companions with  $r_p = 0.1 - 1 \text{ Mpc}$  does depend on stellar mass – the effect is clearly much stronger for the most massive galaxies. However, there is again no evidence that AGN activity is triggered by the presence of a close companion in the way seen for star-formation activity at all stellar masses. We find similar trends when we split our AGN sample by a structural parameter such as the concentration index  $C$ . There is stronger intermediate scale suppression for more concentrated galaxies, but no evidence for significant triggering by close companions in any of our subsamples.



**Figure 3.** Average counts of galaxies in the photometric sample to an  $r$ -band limiting magnitude of  $r_{\text{lim}} = 20$  within a given projected radius  $r_p$  from the star-forming galaxies (left) and from the AGN (right). Different symbols are for star-forming galaxies in different intervals of  $\log_{10} SFR/M_*$  or for AGN in different intervals of  $\log_{10}(L[\text{O III}]/M_{\text{BH}})$ , as indicated.

Our goal in this paper is to understand whether there is a connection between interactions, enhanced star formation, and enhanced AGN activity for SDSS galaxies. In Paper I, we argued that there is a clear connection between galaxy interactions and enhanced star formation. We also argued that galaxy interactions are not only sufficient but also *necessary* to trigger the strongest starbursts. In K03, we demonstrated that powerful AGN have significantly younger stellar populations than non-AGN of the same stellar mass. Clearly, there is a connection between interactions and enhanced star formation, and there is a connection between strong AGN activity and enhanced star formation. The third link, a connection between interactions and strong AGN activity, appears to be missing.

To illustrate this more clearly, we have created subsamples of AGN and high  $S/N$  star-forming galaxies that are closely matched in redshift, stellar mass and concentration index  $C$ . This is illustrated in detail in Figure 6. As can be seen, the full star-forming and AGN samples differ substantially in their distributions of both stellar mass and concentration index. We have shown that the enhancement functions are quite strongly dependent on these two parameters. Thus, if we want to make a *direct* comparison between star-forming galaxies and AGN, we need to create matched subsamples. We can then investigate whether these matched subsamples show identical trends in star formation enhancement as a function of neighbour distance. Our results are shown in Figure 7. Because the luminosities of the higher-ionization emission lines are strongly affected by the central source, star formation rates cannot be estimated very accurately for AGN. We focus instead on the  $\text{H}\alpha$  luminosity of a galaxy normalized to its stellar mass  $M_*$ . As discussed in K03,  $\text{H}\alpha$  line luminosities are very similar in AGN and in

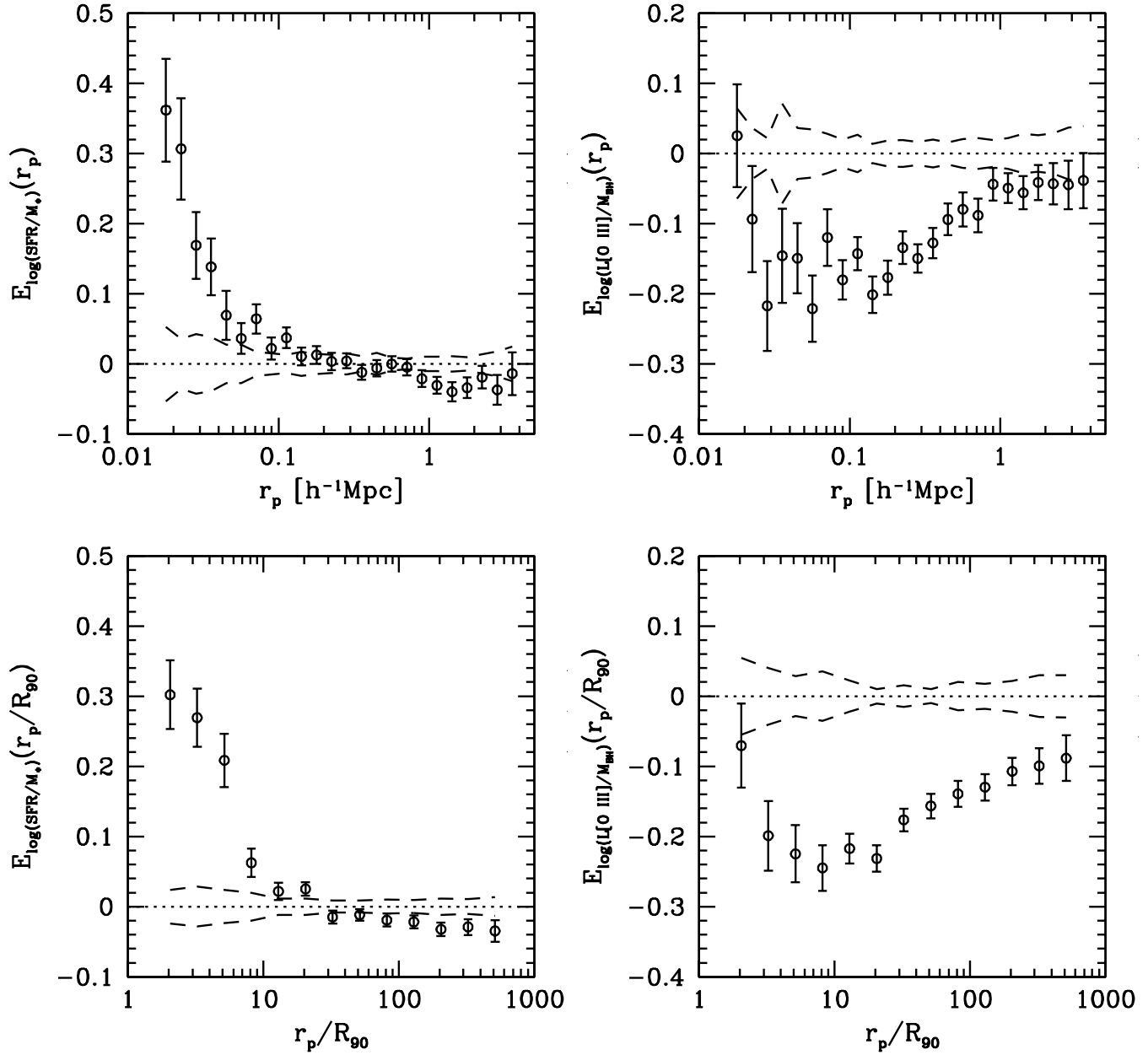
samples of star-forming galaxies that are matched in 4000 Å break strength, proving that most of the  $\text{H}\alpha$  emission arises from  $\text{H II}$  regions in both cases.

Figure 7 shows that on small scales, the behaviour of this indicator as a function of scaled separation is the same in the star-forming galaxies and in the AGN. This suggests that interactions are regulating star formation rates in our sample of AGN in exactly the same way as in our sample of star-forming galaxies! In Figure 8, we plot the enhancement in  $L[\text{O III}]/M_{\text{BH}}$  for the AGN contained in the matched sample. The suppression in nuclear activity level at intermediate scales is no longer quite as strong as in our full sample, because the AGN in the matched sample have significantly lower stellar masses and concentrations. However, we still do not see any significant trend for nuclear activity to increase as the separation between the galaxy and its neighbours gets smaller. We conclude that, unlike enhanced star formation, accretion onto the black hole is not directly connected to interactions for local AGN.

## 4 CONCLUSIONS

The basic conclusion of this paper is very simple. A strong connection between galaxy interactions and enhanced star formation is found no matter what statistic we employ. However, we fail to find any corresponding relation between enhanced AGN activity and interactions. The interpretation of what this implies for the starburst-AGN connection is far from obvious.

We know from previous work (e.g. Kauffmann et al. 2003, ; K03) that galaxies with powerful AGN tend to have younger-than-average stellar populations. K03 found that AGN of all luminosities reside almost exclusively in massive



**Figure 4.** Enhancement in  $\log_{10} SFR/M_*$  for high S/N star-forming galaxies (left) and in  $\log_{10} L[O \text{ III}]/M_{BH}$  for AGN (right), as a function of the projected separation  $r_p$  (top) and as a function of the scaled separation  $r_p/R_{90}$  (bottom). Here  $r < 17.6$  for the central star-forming galaxies and AGN, while  $r < 19.0$  for the reference sample of galaxies from the photometric catalogue.

galaxies and have distributions of sizes, stellar surface mass densities and concentrations that are similar to those of ordinary galaxies of the same mass. The hosts of the AGN with high  $[O \text{ III}]$  luminosities, on the other hand, have much younger mean stellar ages than “normal” galaxies of the same mass. This establishes that there is a physical connection between accretion onto the central black hole and the presence of young stars in the inner galaxy.

There is also a clear physical connection between galaxy interactions and enhanced levels of star formation. This is

true not only for “normal” galaxies, but also for the host galaxies of the AGN in our samples. Figure 7 shows that star formation rates in AGN hosts with a close companion are enhanced in exactly the same way as in normal star-forming galaxies. However, we consistently fail to find any evidence that the black hole accretion rate, as measured by the quantity  $L[O \text{ III}]/M_{BH}$ , increases if a galaxy has a close companion.

These results are summarized in Figure 9. This plot shows how star formation in AGN is enhanced in the plane

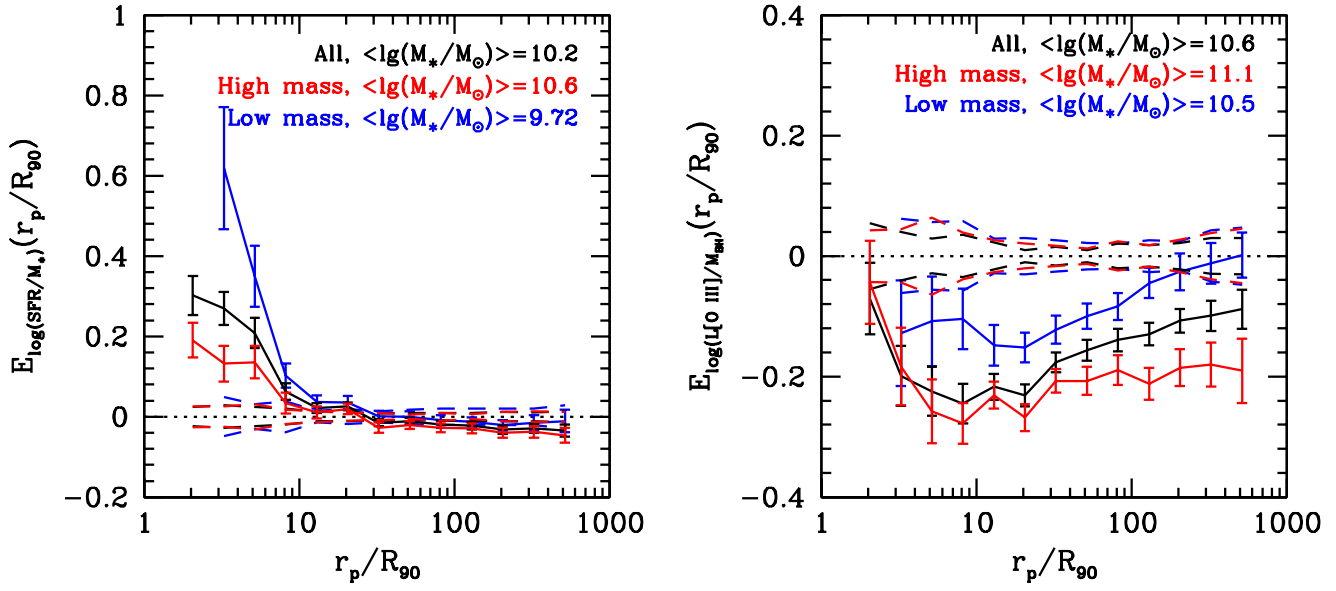


**Figure 5.** Enhancement in  $\log_{10} SFR/M_*$  for high S/N star-forming galaxies (left) and in  $\log_{10} L[O III]/M_{BH}$  for AGN (right), as a function of the scaled separation  $r_p/R_{90}$ , for objects in the different stellar mass ranges as indicated.

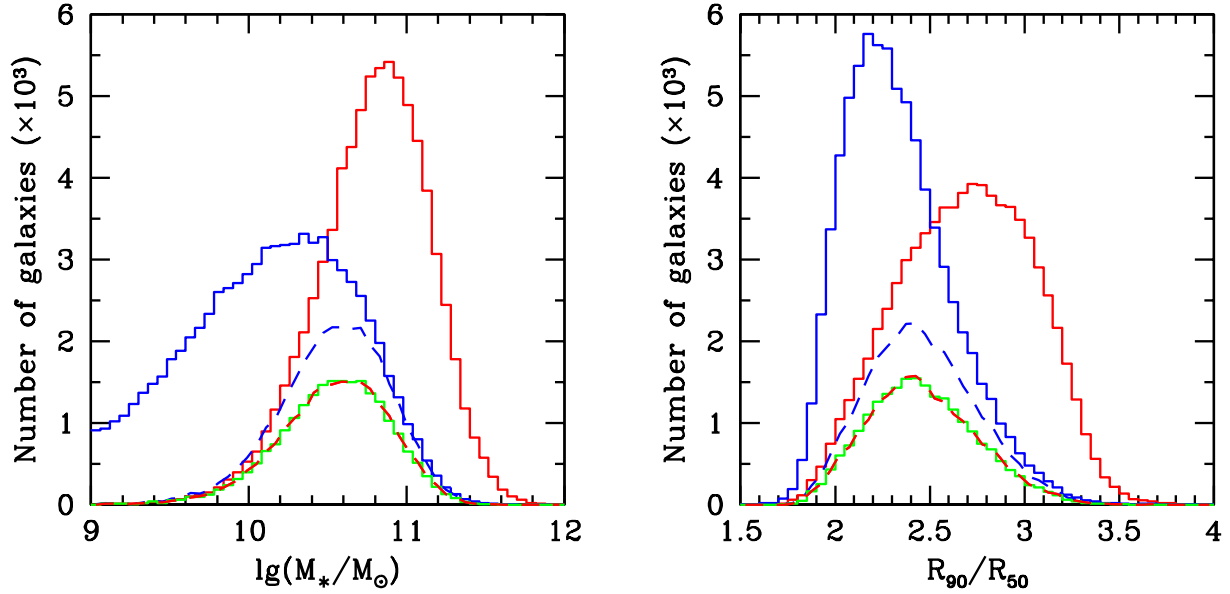


**Figure 6.** Distribution of stellar mass (left) and concentration index (right) for the full star-forming sample (blue solid line), the full AGN sample (red solid line), the star-forming sample matched to AGN in redshift, stellar mass and concentration (blue dashed line), and the AGN matched to star-forming galaxies in the same properties (red dashed line). The green solid line is also for the matched star-forming sample, but is normalized as to have the same total number of objects as the matched AGN sample.

of accretion rate ( $\log L[O III]/M_{BH}$ ) versus projected separation between the AGN and its neighbours. Results are shown for AGN that are closely matched to high S/N star-forming galaxies in redshift, stellar mass and concentration index. Each bin is colour-coded according to the average value of  $\log L(H\alpha)/M_*$  for all the AGN that fall into the given range

in  $\log L[O III]/M_{BH}$ , weighted by the true number of companions at the projected distance  $r_p$ . This weighted average value of  $\log L(H\alpha)/M_*$  is then scaled by the mean value for the sample as a whole. In the upper bar, the scaled, weighted average value of  $\log(H\alpha)/M_*$  is plotted as a function of projected separation for the same sample of AGN. This is thus

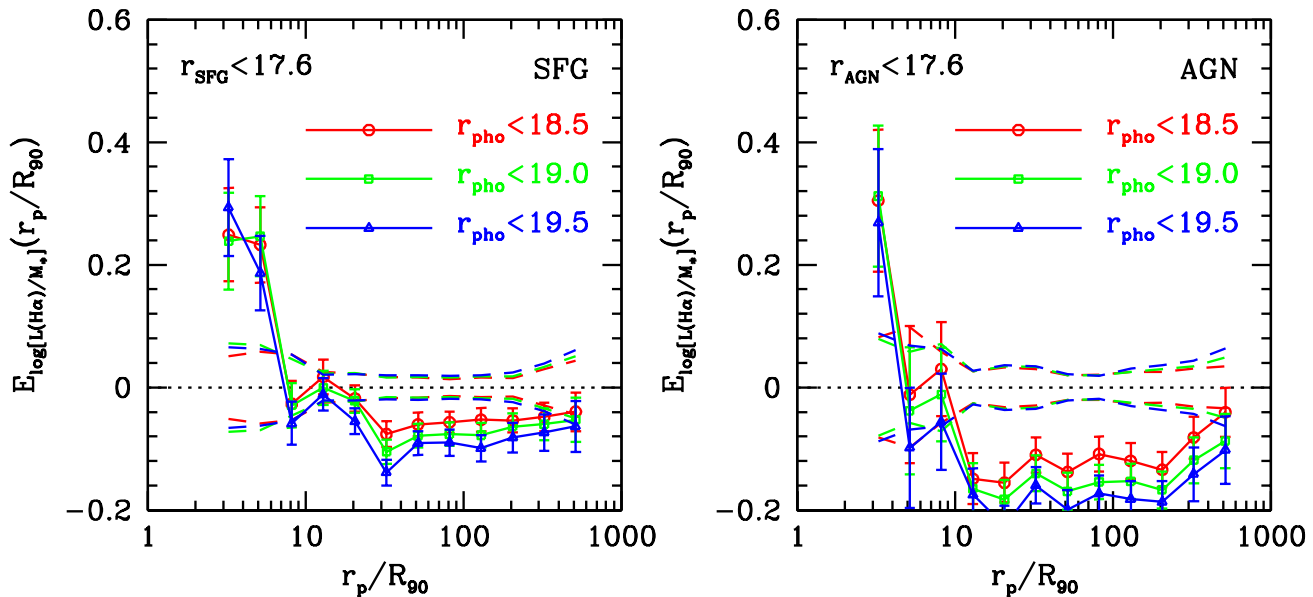


**Figure 7.** Enhancement in  $\log_{10} L(H\alpha)/M_*$  as a function of the scaled separation  $r_p/R_{90}$ , for high S/N star-forming galaxies (left) and for AGN (right). The AGN and star-forming galaxy samples are matched with each other in redshift, stellar mass and concentration index. The limiting magnitude of AGN and star-forming galaxies is fixed at  $r = 17.6$ , but the apparent magnitude limit of the reference galaxy sample is varied as indicated.

the average of the 2-D plot over all accretion rates at each companion distance.

The enhancement in star formation as a function of  $L[O\ III]/M_{BH}$  is clearly seen in this diagram. It is also clear from Figure 9 that the average value of  $L[O\ III]/M_{BH}$  in our sample has no dependence on neighbour distance. The apparent narrowing in the distribution at low values of the scaled separation is simply the result of poorer sample statistics. Finally, it is striking that the degree to which star formation is enhanced as a function of projected separation between the AGN and its companions is considerably weaker than the enhancement that occurs as the black hole accretion rate increases. This point can be seen by comparing the upper bar in Figure 9 with the main panel.

These results lead us to the conclusion that star formation enhancement due to a close companion and star formation enhancement due to an accreting black hole are *two separate and distinct events*. These two events may be part of the same underlying physical process (such as a merger), provided they are well separated in time. In this case, accretion onto the black hole and its associated star formation would occur only after the two interacting galaxies have already merged.

In a recent paper, Yuan et al (2007, in preparation) have studied starburst and AGN activity in infrared-selected galaxies, including ULIRGs. These authors study how the relative fraction of objects classified as starburst or AGN change as the merger event progresses. They find that there is no significant change in fraction of galaxies with AGN activity until the two galactic nuclei have merged. The single nucleus post-merger phase is divided into three classes, according to the K-band core-to-total ratio and morphology. The authors find that for ULIRGS there is a particular stage

(the “diffuse merger” stage) where the nuclei have merged but not yet formed a core, where there is a substantial rise in composite HII-AGN activity. Once the core forms (the so-called “compact merger” stage), this composite activity changes into mostly pure Seyfert activity.

These results appear to support the hypothesis that there is a significant time delay between the onset of the interaction and the phase in which the black hole is able to accrete. This delay hypothesis can be tested by using empirical measures of galaxy morphology that are more sensitive to the later stages of the merging event. Examples include asymmetry indices (Abraham et al. 1996; Conselice et al. 2000) or the “lopsidedness” parameter (Reichard et al. 2007).

A major caveat in all the analysis presented in this paper is the assumption that the extinction-corrected  $[O\ III]$  luminosity is a reasonably robust indicator of the bolometric luminosity of the central black hole. This is the only indicator of accretion that is available to us for our sample of AGN from the Sloan Digital Sky Survey. It will be extremely important to check the results presented in this paper using indicators of AGN activity at other wavelengths.

## ACKNOWLEDGEMENTS

CL is supported by the Joint Postdoctoral Programme in Astrophysical Cosmology of Max Planck Institute for Astrophysics and Shanghai Astronomical Observatory. CL and YPJ are supported by NSFC (10533030, 0742951001), by the Knowledge Innovation Program of CAS (No. KJCX2-YW-T05), and by 973 Program (No.2007CB815402). CL, GK and SW would like to thank the hospitality and stimulat-



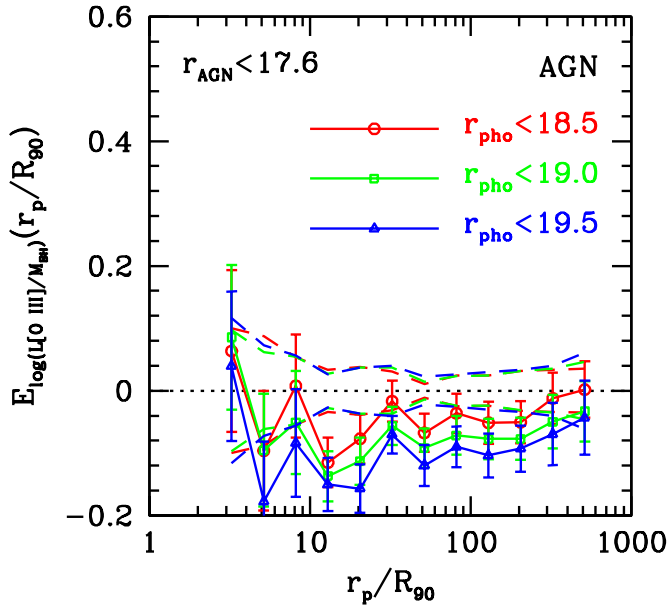


**Figure 8.** Enhancement in  $\log_{10} L[\text{O III}]/M_{BH}$  as a function of the scaled separation  $r_p/R_{90}$ , for AGN that are closely matched to the high  $S/N$  star-forming galaxies in redshift, stellar mass and 4000 Å break index  $D_{4000}$ . The limiting magnitude of the AGN sample is fixed at  $r_{AGN} = 17.6$ , but the apparent magnitude limit for the reference galaxies is varied as indicated.

ing atmosphere of the Aspen Center for Physics while this work was being completed and Roderik Overzier for useful discussions.

Funding for the SDSS and SDSS-II has been provided by the Alfred P. Sloan Foundation, the Participating Institutions, the National Science Foundation, the U.S. Department of Energy, the National Aeronautics and Space Administration, the Japanese Monbukagakusho, the Max Planck Society, and the Higher Education Funding Council for England. The SDSS Web Site is <http://www.sdss.org/>. The SDSS is managed by the Astrophysical Research Consortium for the Participating Institutions. The Participating Institutions are the American Museum of Natural History, Astrophysical Institute Potsdam, University of Basel, Cambridge University, Case Western Reserve University, University of Chicago, Drexel University, Fermilab, the Institute for Advanced Study, the Japan Participation Group, Johns Hopkins University, the Joint Institute for Nuclear Astrophysics, the Kavli Institute for Particle Astrophysics and Cosmology, the Korean Scientist Group, the Chinese Academy of Sciences (LAMOST), Los Alamos National Laboratory, the Max-Planck-Institute for Astronomy (MPIA), the Max-Planck-Institute for Astrophysics (MPA), New Mexico State University, Ohio State University, University of Pittsburgh, University of Portsmouth, Princeton University, the United States Naval Observatory, and the University of Washington.

## REFERENCES

Abraham R. G., van den Bergh S., Glazebrook K., Ellis

- R. S., Santiago B. X., Surma P., Griffiths R. E., 1996, *ApJS*, 107, 1
- Adelman-McCarthy J. K., Agüeros M. A., Allam S. S., Anderson K. S. J., Anderson S. F., Annis J., Bahcall N. A., Baldry I. K., et al., 2006, *ApJS*, 162, 38
- Balogh M. L., Morris S. L., Yee H. K. C., Carlberg R. G., Ellingson E., 1999, *ApJ*, 527, 54
- Barton E. J., Arnold J. A., Zentner A. R., Bullock J. S., Wechsler R. H., 2007, *ArXiv e-prints*, 708
- Bower R. G., Benson A. J., Malbon R., Helly J. C., Frenk C. S., Baugh C. M., Cole S., Lacey C. G., 2006, *MNRAS*, 370, 645
- Brinchmann J., Charlot S., White S. D. M., Tremonti C., Kauffmann G., Heckman T., Brinkmann J., 2004, *MNRAS*, 351, 1151
- Cattaneo A., 2001, *MNRAS*, 324, 128
- Cattaneo A., Blaizot J., Devriendt J., Guiderdoni B., 2005, *MNRAS*, 364, 407
- Conselice C. J., Bershadsky M. A., Jangren A., 2000, *ApJ*, 529, 886
- Croton D. J., Springel V., White S. D. M., De Lucia G., Frenk C. S., Gao L., Jenkins A., Kauffmann G., et al., 2006, *MNRAS*, 365, 11
- Dahari O., 1984, *AJ*, 89, 966
- Dahari O., 1985, *ApJS*, 57, 643
- Di Matteo T., Croft R. A. C., Springel V., Hernquist L., 2003, *ApJ*, 593, 56
- Ferrarese L., Merritt D., 2000, *ApJL*, 539, L9
- Fuentes-Williams T., Stocke J. T., 1988, *AJ*, 96, 1235
- Gebhardt K., Bender R., Bower G., Dressler A., Faber S. M., Filippenko A. V., Green R., Grillmair C., et al., 2000, *ApJL*, 539, L13
- Granato G. L., Silva L., Monaco P., Panuzzo P., Salucci P., De Zotti G., Danese L., 2001, *MNRAS*, 324, 757
- Grogin N. A., et al., 2005, *ApJ*, 627, L97
- Heckman T. M., Kauffmann G., Brinchmann J., Charlot S., Tremonti C., White S. D. M., 2004, *ApJ*, 613, 109
- Heckman T. M., Ptak A., Hornschemeier A., Kauffmann G., 2005, *ApJ*, 634, 161
- Hopkins P. F., Hernquist L., Martini P., Cox T. J., Robertson B., Di Matteo T., Springel V., 2005, *ApJL*, 625, L71
- Kang X., Jing Y. P., Mo H. J., Börner G., 2005, *ApJ*, 631, 21
- Kauffmann G., Haehnelt M., 2000, *MNRAS*, 311, 576
- Kauffmann G., Heckman T. M., Tremonti C., Brinchmann J., Charlot S., White S. D. M., Ridgway S. E., Brinkmann J., et al., 2003, *MNRAS*, 346, 1055
- Keel W. C., Kennicutt R. C., Jr., Hummel E., van der Hulst J. M., 1985, *AJ*, 90, 708
- Koulouridis E., Plionis M., Chavushyan V., Dultzin-Hacyan D., Krongold Y., Goudis C., 2006, *ApJ*, 639, 37
- Li C., Kauffmann G., Heckman T., Jing Y. P., White S. D. M., 2007, *arXiv*, 711, arXiv:0711.3792
- Li C., Kauffmann G., Wang L., White S. D. M., Heckman T. M., Jing Y. P., 2006, *MNRAS*, 373, 457
- Mihos J. C., Hernquist L., 1996, *ApJ*, 464, 641
- Miller C. J., Nichol R. C., Gómez P. L., Hopkins A. M., Bernardi M., 2003, *ApJ*, 597, 142
- Negroponte J., White S. D. M., 1983, *MNRAS*, 205, 1009
- Petrosian A. R., 1982, *Afz*, 18, 548
- Reichard T. A., Heckman T. M., Rudnick G., Brinchmann J., Kauffmann G., 2007, *arXiv*, 710, arXiv:0710.0589

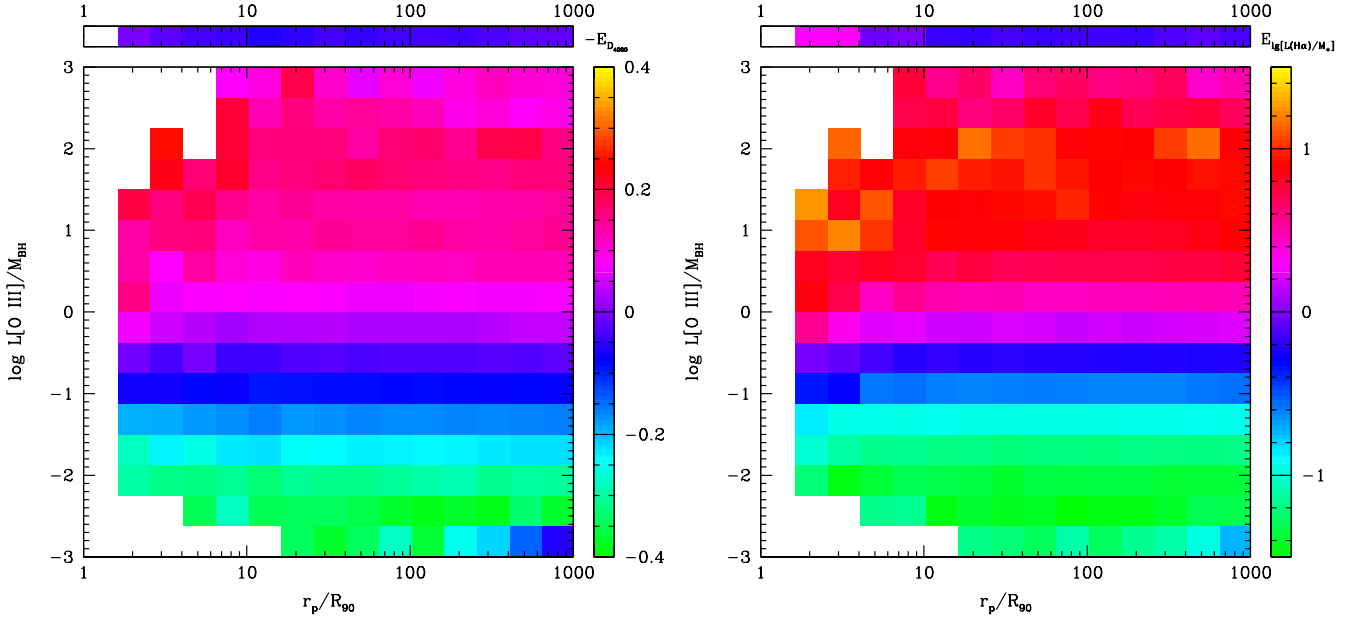


**Figure 9.** The enhancement in star formation for AGN is plotted in the plane of accretion rate ( $L[\text{O III}]/M_{\text{BH}}$ ) versus the projected separation between an AGN host and its neighbours (scaled to the 90% light radius of the host). Results are shown for AGN that are closely matched to high  $S/N$  star-forming galaxies in redshift, stellar mass and concentration index. Each bin is colour-coded according to the average value of  $-D_{4000}$  (the left-hand panel) or  $\log L(\text{H}\alpha)/M_*$  (the right-hand panel) for all the AGN that fall into the given range in  $\log L[\text{O III}]/M_{\text{BH}}$ , weighted by the true number of companions at projected distance  $r_p$ . This weighted average value of  $-D_{4000}$  or  $\log L(\text{H}\alpha)/M_*$  is then scaled by the mean value for the sample as a whole. In each panel, the colour coding is indicated by the bar on the right. The bar at the top shows the scaled, weighted average value of  $-D_{4000}$  or  $\log L(\text{H}\alpha)/M_*$  as a function of projected separation for the same sample of AGN. This is simply the vertical average of the data in the main panel.

- Schmitt H. R., 2001, *AJ*, 122, 2243  
 Serber W., Bahcall N., Ménard B., Richards G., 2006, *ApJ*, 643, 68  
 Tremaine S., Gebhardt K., Bender R., Bower G., Dressler A., Faber S. M., Filippenko A. V., Green R., et al., 2002, *ApJ*, 574, 740  
 Virani S. N., De Robertis M. M., VanDalsen M. L., 2000, *AJ*, 120, 1739  
 Waskett T. J., Eales S. A., Gear W. K., McCracken H. J., Lilly S., Brodwin M., 2005, *MNRAS*, 363, 801  
 Wyithe J. S. B., Loeb A., 2002, *ApJ*, 581, 886  
 York D. G., Adelman J., Anderson Jr. J. E., Anderson S. F., Annis J., Bahcall N. A., Bakken J. A., Barkhouser R., et al., 2000, *AJ*, 120, 1579

This paper has been typeset from a  $\text{\LaTeX}$  file prepared by the author.